**Atmospheric
Chemistry
and Physics**

Nitrogen deposition to the United States: distribution, sources, and processes

L. Zhang[1,2], D. J. Jacob[1,2], E. M. Knipping[3], N. Kumar[4], J. W. Munger[1,2], C. C. Carouge[2], A. van Donkelaar[5], Y. X. Wang[6], and D. Chen[7]

[1]Department of Earth and Planetary Sciences, Harvard University, Cambridge, MA, USA
[2]School of Engineering and Applied Sciences, Harvard University, Cambridge, MA, USA
[3]Electric Power Research Institute, Washington, DC, USA
[4]Electric Power Research Institute, Palo Alto, CA, USA
[5]Department of Physics and Atmospheric Science, Dalhousie University, Halifax, Canada
[6]Ministry of Education Key Laboratory for Earth System Modeling, Center for Earth System Science, Institute for Global Change Studies, Tsinghua University, Beijing, China
[7]Department of Atmospheric and Oceanic Sciences, University of California, Los Angeles, CA, USA

Correspondence to: L. Zhang (linzhang@fas.harvard.edu)

Abstract. We simulate nitrogen deposition over the US in 2006–2008 by using the GEOS-Chem global chemical transport model at $1/2° \times 2/3°$ horizontal resolution over North America and adjacent oceans. US emissions of NO_x and NH_3 in the model are 6.7 and $2.9\,Tg\,N\,a^{-1}$ respectively, including a 20 % natural contribution for each. Ammonia emissions are a factor of 3 lower in winter than summer, providing a good match to US network observations of NH_x ($\equiv NH_3$ gas + ammonium aerosol) and ammonium wet deposition fluxes. Model comparisons to observed deposition fluxes and surface air concentrations of oxidized nitrogen species (NO_y) show overall good agreement but excessive wintertime HNO_3 production over the US Midwest and Northeast. This suggests a model overestimate N_2O_5 hydrolysis in aerosols, and a possible factor is inhibition by aerosol nitrate. Model results indicate a total nitrogen deposition flux of $6.5\,Tg\,N\,a^{-1}$ over the contiguous US, including 4.2 as NO_y and 2.3 as NH_x. Domestic anthropogenic, foreign anthropogenic, and natural sources contribute respectively 78 %, 6 %, and 16 % of total nitrogen deposition over the contiguous US in the model. The domestic anthropogenic contribution generally exceeds 70 % in the east and in populated areas of the west, and is typically 50–70 % in remote areas of the west. Total nitrogen deposition in the model exceeds $10\,kg\,N\,ha^{-1}\,a^{-1}$ over 35 % of the contiguous US.

1 Introduction

Atmospheric input of reactive nitrogen (often called "fixed nitrogen") to ecosystems has increased by more than a factor of 3 globally due to human activity, significantly perturbing the global nitrogen cycle (Vitousek et al., 1997; Galloway et al., 2004). Adverse effects may include soil acidification (Bowman et al., 2008), eutrophication (Bouwman et al. 2002), and a reduction in plant biodiversity (Stevens et al., 2004). Increased nitrogen deposition may enhance CO_2 uptake by the land and ocean, though the climate benefit would be offset by associated N_2O emission (Reay et al., 2008). The US Environmental Protection Agency (EPA) is presently developing secondary air quality standards for protection of ecosystems against the detrimental effects of nitrogen deposition (US EPA, 2008). This requires a better understanding of nitrogen deposition over the US in its various forms and including contributions from sources both natural and anthropogenic, foreign and domestic. We use here a nested version of the global GEOS-Chem chemical transport model (CTM) to address these issues.

The anthropogenic contribution to nitrogen deposition is mainly driven by emissions of nitrogen oxide radicals ($NO_x \equiv NO + NO_2$) and ammonia (NH_3). These species also have natural sources. NO_x is emitted to the atmosphere by

combustion, microbial activity in soils, and lightning. In the atmosphere, NO_x is oxidized to nitric acid (HNO_3) and organic nitrates on a time scale of less than a day. These can be deposited to ecosystems by direct uptake (dry deposition). In addition, HNO_3 is highly soluble in water and is scavenged efficiently by precipitation (wet deposition). NH_3 is emitted to the atmosphere by agriculture (mostly animal husbandry and fertilizer use), natural terrestrial and marine ecosystems, and fires. NH_3 in the atmosphere can combine with H_2SO_4 (from SO_2 oxidation) and HNO_3 to produce ammonium sulfate and nitrate particles. Dry deposition is fast for gaseous NH_3 but slow for ammonium particles, while wet deposition is efficient for both.

The lifetime of fixed nitrogen in the atmosphere is sufficiently short that most of the nitrogen deposition for a large country such as the US is expected to be of domestic origin. However, transboundary transport including on intercontinental scales can also be significant (Asman et al., 1998; Dentener et al., 2006; Sanderson et al. 2008). A number of studies have estimated an export efficiency of 20–30 % for nitrogen oxides ($NO_y \equiv NO_x$ and its oxidation products) emitted in the US (Jacob et al., 1993; Kasibhatla et al., 1993; Liang et al., 1998; Li et al., 2004). No analysis has been conducted so far on the relative contributions from domestic, foreign, and natural sources to the different forms of nitrogen deposition over the US.

Here we use a nested continental scale version of the GEOS-Chem global CTM (Y. Wang et al., 2004; Chen et al., 2009) with horizontal resolution of $1/2° \times 2/3°$ over North America and $2° \times 2.5°$ for the rest of the world. Three-year GEOS-Chem simulations (2006–2008) are conducted to quantify the sources and processes contributing to nitrogen deposition to the US. We present an extensive evaluation for 2006 with surface measurements of wet deposition fluxes, HNO_3 and aerosol concentrations, and satellite observations of NO_2. We quantify the contributions to nitrogen deposition from wet vs. dry processes and from individual nitrogen species. We also separate the contributions from domestic anthropogenic, foreign anthropogenic, and natural sources.

2 The GEOS-Chem nested-grid model

2.1 General description

The GEOS-Chem 3-D global chemical transport model (v8-02-03; http://geos-chem.org) was originally described by Bey et al. (2001) and Park et al. (2004). The model here is driven by GEOS-5 assimilated meteorological data for 2006-2008 from the NASA Global Modeling and Assimilation Office (GMAO). The GEOS-5 data are available with a temporal resolution of 6 hours (3 hours for surface variables and mixing depths), a horizontal resolution of $1/2°$ latitude by $2/3°$ longitude, and 72 vertical layers from the surface to 0.01 hPa. The lowest 5 layers are centered at 70, 200, 330, 470,

and 600 m for a column above sea level. We use a nested version of GEOS-Chem (Wang et al., 2004; Chen et al., 2009) with the native $1/2° \times 2/3°$ horizontal resolution over North America and adjacent oceans (140°–40° W, 10°–70° N), and $2° \times 2.5°$ horizontal resolution for the rest of the world. Zhang et al. (2011) previously used the exact same model to estimate policy-relevant background ozone in surface air over the US.

The model includes a detailed simulation of tropospheric ozone-NO_x-hydrocarbon-aerosol chemistry, as recently described for example by Mao et al. (2010). Formation of organic nitrates from the oxidation of biogenic isoprene emitted by vegetation can be a significant sink for NO_x in the model (Horowitz et al., 1998). We assume that these isoprene nitrates are removed by wet and dry deposition at the same deposition velocity as HNO_3 and do not regenerate NO_x. Earlier versions of GEOS-Chem did not explicitly describe isoprene nitrates, treating them instead as HNO_3 (Bey et al., 2001). Here we describe them explicitly in order to compare simulated HNO_3 with observations and to quantify the contribution of isoprene nitrates to dry deposition.

Aerosol and gas-phase chemistry in GEOS-Chem are coupled through gas-aerosol partitioning of semi-volatile species including NH_3 and HNO_3, heterogeneous aerosol chemistry parameterized as reactive uptake coefficients (Jacob, 2000), and aerosol effects on photolysis rates (Martin et al., 2003). Partitioning of total NH_3 and HNO_3 between gas and aerosol phases is estimated with the RPMARES thermodynamic equilibrium model (Binkowski and Roselle, 2003). The reactive uptake coefficients $\gamma_{N_2O_5}$ for N_2O_5 in aerosols are from Evans and Jacob (2005), reduced by a factor of 10 as tested by Macintyre and Evans (2010). The resulting annual mean value of $\gamma_{N_2O_5}$ in surface air over the contiguous US is 0.003, comparable to measured values in the range of 0.0005–0.006 (Brown et al., 2009; Bertram et al., 2009).

We conduct three-year GEOS-Chem simulations for 2006–2008. We first conduct the global simulation at $2° \times 2.5°$ resolution, and archive the output at 3-h temporal resolution for use as boundary conditions in the nested model. Output from the nested model does not affect the global simulation (one-way nesting).

2.2 Deposition

Wet deposition for aerosols follows the scheme described by Liu et al. (2001), with adaptation to soluble gases described by Mari et al. (2000) and Amos et al. (2012). The scheme includes scavenging in convective updrafts as well as in-cloud and below-cloud scavenging from large-scale precipitation. In warm (liquid) clouds with $T > 268$ K, aerosols are assumed to be 100 % incorporated in cloud droplets and gases are partitioned following Henry's law. In mixed (liquid/ice) clouds ($248 < T < 268$ K), where precipitation takes place by riming, aerosols are retained in the rime ice while gases are retained with varying efficiencies (unity for HNO_3 but 0.05 for NH_3;

Table 1. Mean daytime dry deposition velocities over the contiguous US[a].

Species	v_d (cm s^{-1})
NH$_3$	0.65±0.40
Aerosol NH$_4^+$	0.15±0.03
HNO$_3$	2.7±1.5
N$_2$O$_5$	2.7±1.5
Isoprene nitrates	2.7±1.5
NO$_2$	0.36±0.22
PANs[b]	0.32±0.20
alkyl nitrates	0.32±0.20
Aerosol NO$_3^-$	0.15±0.03

[a] Annual mean daytime (10-16 local time) values computed in GEOS-Chem for the ensemble of 1/2°×2/3° grid squares covering the contiguous US and for the midpoint of the lowest grid level (∼70 m above the surface). Standard deviations describe the spatial variability of the annual means.
[b] Peroxyacetyl nitrate (PAN) and higher peroxyacyl nitrates.

Table 2. NO$_x$ and NH$_3$ emissions over the contiguous US[a].

	Source type	Emission (Tg N a^{-1})
NO$_x$	Total	6.7
	Anthropogenic	5.3
	Lightning	0.63
	Soil	0.41
	Aircraft	0.13
	Fertilizer use	0.12
	Open fires	0.055
NH$_3$	Total	2.9
	Anthropogenic	2.3
	Natural	0.56

[a] Annual GEOS-Chem emissions for 2006–2008.

Wang et al. (2008)). In cold (ice) clouds ($T < 248$ K), both aerosols and HNO$_3$ are scavenged with 100 % efficiency (HNO$_3$ is taken up as a monolayer; Abbatt (1997)), while NH$_3$ is not scavenged.

Dry deposition of gases and aerosols is simulated with a standard big-leaf resistance-in-series model (Wesely, 1989). The dry deposition flux F_d out of the lowest model layer (midpoint $z_1 \approx 70$ m above the surface) is calculated as:

$$F_d = n_a C(z_1) v_d(z_1) \tag{1}$$

where n_a (molecules cm^{-3}) is the number density of air, $C(z_1)$ is the mixing ratio of the depositing species at height z_1, and v_d is its deposition velocity (cm s^{-1}) at that height. The deposition velocity is a function of the local meteorological condition and surface type, as given by:

$$v_d(z_1) = (R_a(z_1, z_0) + R_b + R_c)^{-1} \tag{2}$$

Here $R_a(z_1, z_0)$ is the aerodynamic resistance to turbulent transfer from z_1 to the roughness height z_0 close to the surface where turbulence vanishes, R_b is the boundary layer resistance to molecular diffusion from z_0 to the actual surface, and R_c is the canopy or surface uptake resistance.

Table 1 lists the annual mean daytime (10:00–16:00 local time) dry deposition velocities for different species computed in the model over the contiguous US. Values average 2.7±1.5 cm s^{-1} for HNO$_3$, N$_2$O$_5$, and isoprene nitrates; 0.65±0.40 cm s^{-1} for NH$_3$; and 0.15–0.36 cm s^{-1} for aerosols, NO$_2$, peroxyacetyl nitrate (PAN), and other organic nitrates. Other nitrogen species are not significantly removed by dry deposition. Model values are consistent with experimental studies, which report daytime dry deposition velocities to land in the 2–10 cm s^{-1} range for HNO$_3$ (Sievering et

al., 2001; Horii et al., 2005), and in the 0.1–1.0 cm s^{-1} range for PAN (Doskey et al., 2004; Turnipseed et al. 2006; Wolfe et al., 2009). Biosphere-atmosphere exchange of NO$_x$ and NH$_3$ is bi-directional (Sutton et al., 1998; Lerdau et al., 2000; Ellis et al., 2011), but is treated here as uncoupled emission and deposition processes. The fluxes to the surface are parameterized as uni-directional dry deposition, and the fluxes back to the atmosphere are included as part of natural emissions.

2.3 Emissions

A description of NO$_x$ emissions in the model is given in Zhang et al. (2011). We use global anthropogenic emissions of NO$_x$, CO, volatile organic compounds (VOCs), and SO$_2$ from the EDGAR inventory (Olivier and Berdowski, 2001), and global anthropogenic emissions of NH$_3$ from GEIA (Bouwman et al., 1997). The global inventories are replaced with regional emission inventories including EPA NEI-2005 for the US, the CAC inventory for Canada (http://www.ec.gc.ca/pdb/cac/cac_home_e.cfm), BRAVO for Mexico (Kuhns et al., 2005), EMEP for Europe (Vestreng and Klein, 2002), and Zhang et al. (2009) for Asia. The US anthropogenic emissions of NH$_3$ from NEI-2005 are further modified to match surface total reduced nitrogen concentrations as described below. These global and regional inventories are scaled to the simulation year (2006-2008) based on the energy statistics described by van Donkelaar et al. (2008), except for NEI-2005 that is fixed for the year 2005. The model also includes global NO$_x$ emissions from fertilizer use and aircraft based on Yienger and Levy (1995) and Baughcum et al. (1996), respectively.

Natural NO$_x$ sources include lightning, soil, and open fires. NO$_x$ emissions from lightning are computed using the cloud top height parameterization of Price and Rind (1992), and vertically distributed following Pickering et al. (1998). The spatial distribution of lightning flashes is constrained with the 10-yr averaged OTD/LIS satellite observations as described by Sauvage et al. (2007). The NO$_x$
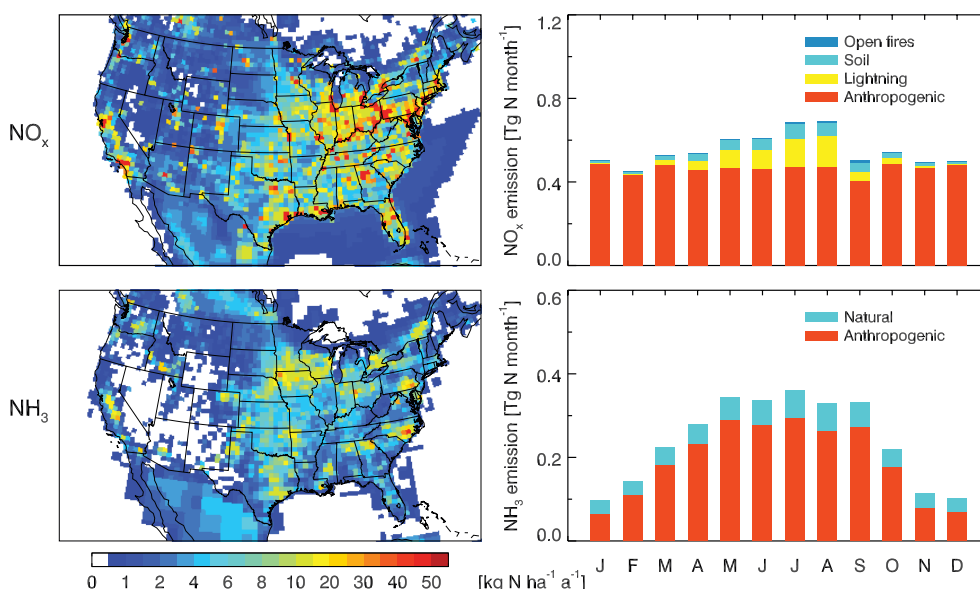
Fig. 1. NO_x and NH_3 emissions in 2006-2008. The left panels show annual total emissions at the $1/2° \times 2/3°$ resolution of GEOS-Chem. The right panels show seasonal variations for each source type over the contiguous US. Annual totals by source type are given in Table 2.
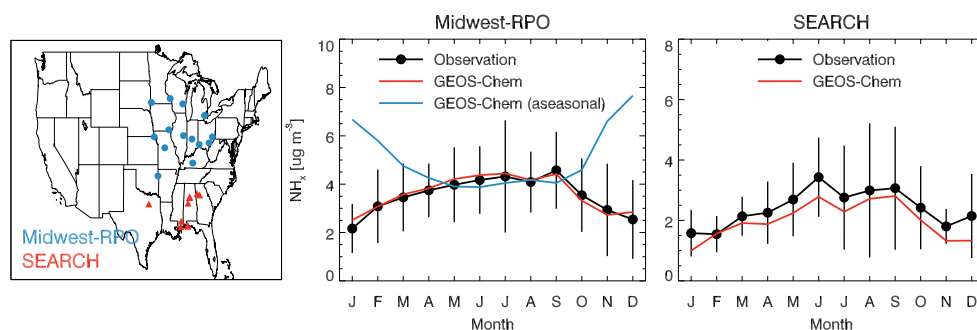

Fig. 2. Atmospheric concentrations of total reduced nitrogen ($NH_x \equiv NH_3 + NH_4^+$) at the Midwest-RPO and SEARCH networks. Site locations are shown in the left panel. Monthly mean concentrations averaged across all sites of each network are shown in the central and right panels. Observations (black) are compared to model results using the NEI NH_3 anthropogenic emissions with no seasonal variation (blue line in the central panel) and with seasonal variation fitted to the Midwest-RPO data (red lines). The Midwest-RPO and SEARCH data are for 2004-2005 and 2006, respectively, and model results are for 2006. Vertical bars represent standard deviations in the observed monthly means for individual sites and years.

yield is estimated to be 500 mol per flash at northern mid-latitudes, and 125 mol per flash in the tropics (Hudman et al., 2007), and this gives a global lightning source of $6 \, Tg \, N \, a^{-1}$ (Martin et al., 2007). Soil NO_x emissions follow the algorithm of Yienger and Levy (1995) with canopy reduction factors (Wang et al., 1998). Open fires emissions are from the monthly GFED-v2 inventory (van der Werf et al., 2006). Natural NH_3 emissions from soil, vegetation, and the oceans are from the GEIA inventory (Bouwman et al., 1997). Biogenic VOC emissions, which are important for the conversion of NO_x to organic nitrates, are from MEGAN (Guenther et al., 2006).

Figure 1 shows the spatial and seasonal distribution of US NO_x emissions and Table 2 gives annual totals from

each source over the contiguous US. Anthropogenic sources ($5.6 \, Tg \, N \, a^{-1}$ including fertilizer use and aircraft) account for 84 % of the total NO_x emissions. Natural sources from lightning, soil, and open fires account for 9.5 %, 6.2 %, and 0.7 %, respectively. Natural contributions peak in summer, accounting for 39 % of US NO_x emissions in July.

Gilliland et al. (2003, 2006) and Pinder et al. (2006) previously found large seasonally varying errors in the US NEI emission inventory for NH_3 by model comparison with observed wet deposition fluxes of ammonium (NH_4^+) and atmospheric concentrations of total reduced nitrogen ($NH_x \equiv NH_3$ gas + ammonium aerosol). Here we use NH_x measurements from two networks (Fig. 2, left panel) to constrain the seasonality of NH_3 emissions: the Midwest Ammonia

Monitoring Project managed by the Midwest Regional Planning Organization (RPO) for 2004–2005 (http://www.ladco.org), and the Southeastern Aerosol Research and Characterization (SEARCH) for 2006 (Edgerton et al., 2006). Figure 2 (central panel) compares observations to model results in a simulation with the August NEI-2005 NH_3 emission applied to the whole year (no seasonality source). Results agree well with measurements in summer but are too high in winter, reflecting a lower NH_3 emission in winter than that in summer, as would be expected in view of the temperature dependence of NH_3 emission (Aneja et al., 2000). We fit monthly scaling factors as observed/simulated concentration ratios to the NEI emissions to correct the discrepancy shown in the central panel of Figure 2 and apply them nationwide. These scaling factors range from 0.9–1 in summer to 0.2–0.4 in winter. Independent comparison of the resulting model to the SEARCH data for 2006 (Fig. 2, right panel) shows good agreement and thus supports these seasonal scaling factors.

Figure 1 shows the spatial and seasonal distribution of US NH_3 emissions with the above scaling factors applied, and Table 2 gives annual totals for each source. Emissions show a broad May-September maximum. The highest emissions are in areas of major livestock operations. Anthropogenic emissions ($2.3\,Tg\,N\,a^{-1}$, 81 %) dominate over natural emissions ($0.56\,Tg\,N\,a^{-1}$, 19 %).

Our NO_x and NH_3 emission estimates can be compared with those of Smith and Mueller (2010), who implemented natural emission inventories into the CMAQ regional model for July 2002. For a model domain ($130°$–$70°$ W, $23°$–$56°$ N) covering the contiguous US and large fractions of Canada and Mexico, they found natural emissions to contribute 44 % of NO_x emissions and 28 % of NH_3 emissions. Our results for July 2006 over the same CMAQ domain are comparable, with natural emission contributions of 40 % for NO_x and 24 % for NH_3. The largest difference is for open fire NO_x emissions, which are a factor of 5 higher in Smith et al. (2010). The GFED-v2 fire emissions used in GEOS-Chem indicate that dry mass burned over the CMAQ domain was a factor of 4 higher in July 2002 than in July 2006, mostly due to large fires in eastern Canada in 2002.

3 Deposition patterns and surface concentrations

Figure 3a–c compares simulated and observed sulfate, ammonium, and nitrate wet deposition fluxes over the US and Canada for 2006. The observations are from the 251 sites of the National Atmospheric Deposition Program/National Trends Network (NADP/NTN; data available at https://nadp.isws.illinois.edu/) for the US, and 26 sites of the Canadian Air and Precipitation Monitoring Network (CAPMoN; data available at http://www.on.ec.gc.ca/natchem/index.aspx) for Canada. We use sulfate as a check on the wet deposition processes in the model since the SO_2 source from coal combustion is well constrained by stack measurements. We summa-

rize the comparison between the model (M) and observations (O) using the correlation coefficient, the normalized mean bias (NMB) computed as $NMB = \dfrac{\sum_{i=1}^{N}(M_i - O_i)}{\sum_{i=1}^{N} O_i}$ for the N sites, and the mean normalized bias $MNB = \dfrac{1}{N}\sum_{i=1}^{N}(M_i - O_i)/O_i$. The NMB estimates the mean offset between the model and observations, while MNB provides a sensitive evaluation of the model performance for observed low values.

For all three species the model shows strong correlations with observations, no significant annual biases, and little seasonal bias. MNB and NMB generally agree within a few percent, except for some seasonal cases where MNB is $\sim$20 % higher due to model overestimates of very low observations. Wet deposition generally peaks in summer for all three species, in the case of sulfate and nitrate because of higher SO_2 and NO_x oxidant concentrations, and in the case of ammonium because of higher ammonia emissions. The summer peak of nitrate wet deposition is particularly pronounced around the Gulf of Mexico where it reflects the seasonal maxima in both lightning and precipitation. Simulated nitrate wet deposition peaks in Michigan and southeastern Canada in winter, caused by transport of HNO_3 and nitrate aerosols produced mostly from N_2O_5 hydrolysis. This winter maximum is less pronounced in the observations, suggesting that N_2O_5 hydrolysis in the model may be too fast as discussed further below. The model does not capture the observed high values of ammonium wet deposition in the upper Midwest, as previously noted by Fisher et al. (2011), likely because of regional underestimate of emissions. Our national scaling factors are derived from NH_x measurements in the east (Fig. 2), and may fail to correct the regional emissions in the upper Midwest.

No routine direct measurements of dry deposition fluxes are available at US sites. However, the Clean Air Status and Trends Network (CASTNet) makes weekly integrated measurements of gas-phase HNO_3 concentrations from which dry deposition fluxes can be estimated using modeled dry deposition velocities (Clarke et al., 1997). Figure 4 compares annual mean HNO_3 concentrations from CASTNet with GEOS-Chem results in 2006. The model has a mean positive bias of 69 %, which is due in part to the vertical gradient of concentrations between the lowest model grid-point ($z_1 = 70\,m$) and the CASTNet measurement altitude ($z_C = 10\,m$). This gradient can be quantified from the resistance-in-series formulation for dry deposition used in GEOS-Chem. We re-express the deposition flux in Eq. (1) as

$$F_d = n_a C(z_1) v_d(z_1) = n_a \frac{C(z_1) - C(z_C)}{R_a(z_1, z_C)} \qquad (3)$$

where $R_a(z_1, z_C)$ is the aerodynamic resistance between z_1 and z_C. In the GEOS-Chem resistance-in-series formulation the aerodynamic resistance is calculated between z_1 and z_0
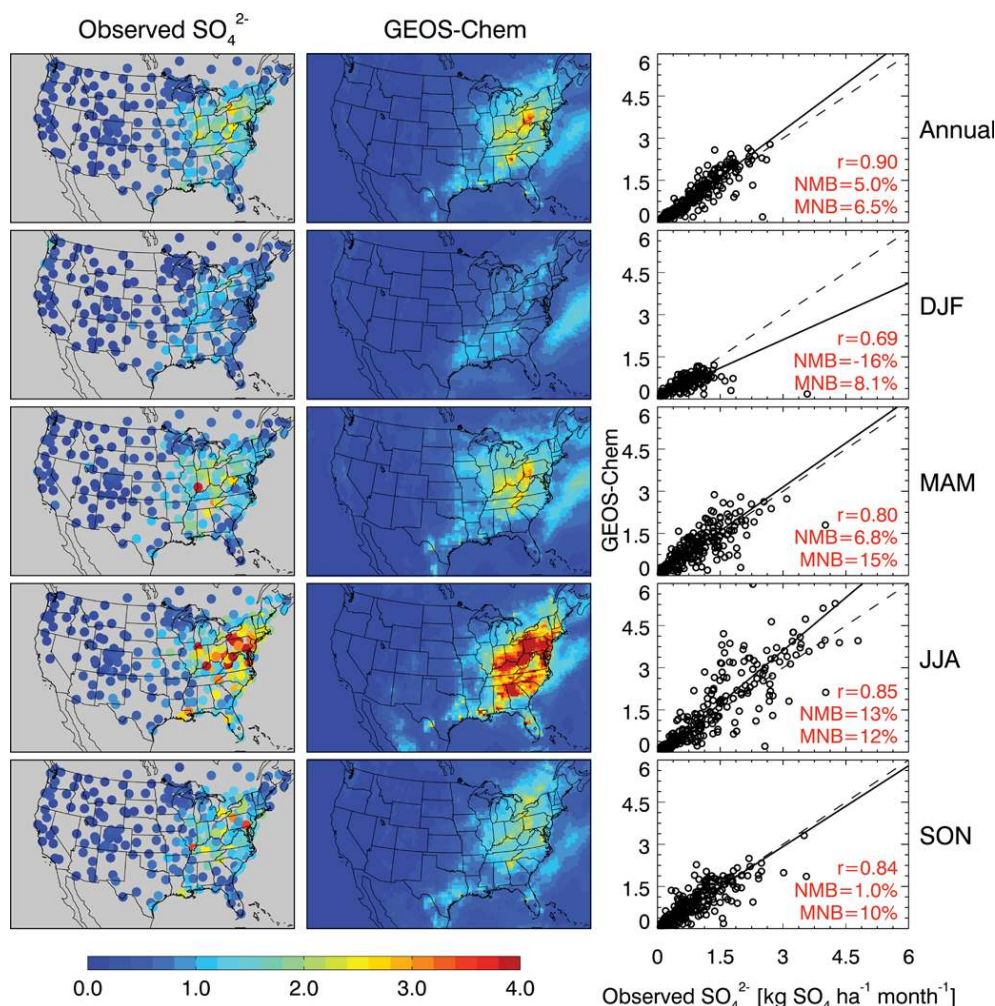
Fig. 3a. Annual and seasonal mean sulfate wet deposition fluxes measured at NADP and CAPMoN sites (left panels) and simulated by GEOS-Chem (central panels) in 2006. The right panels show scatter-plots of simulated versus observed values at individual sites. Correlation coefficients (r), normalized mean biases (NMB), and mean normalized biases (MNB) are shown inset. Reduced-major-axis regression lines (solid) and the 1:1 lines (dash) are also shown.

(Eq. 2) using Monin-Obukhov similarity with momentum, and the same expression can be used to calculate the aerodynamic resistance between z_1 and z_C:,

$$R_a(z_1, z_C) = \int_{z_C}^{z_1} \frac{\Phi(\zeta)}{ku*\zeta} d\zeta \qquad (4)$$

Here $\zeta = z/L$, L is the Monin-Obukhov length that is function of the local surface fluxes of momentum and sensible heat, Φ is a stability-dependent function (Businger et al., 1971), u^* is the friction velocity, and k is the von Karman constant. The implied model concentration at the CASTNet height z_C is related to the concentration at the lowest model gridpoint z_1 by:

$$C(z_C) = (1 - R_a(z_1, z_C) v_d(z_1)) C(z_1) \qquad (5)$$

We retrieved $(1 - R_a(z_1, z_C) v_d(z_1))$ locally from GEOS-Chem, and applied it to $C(z_1)$ following Eq. (5). The right panel of Figure 4 shows the implied model HNO$_3$ concentrations at 10 m. They are on average 30 %–40 % lower than those at 70 m, and the normalized mean bias relative to the CASTNet measurements reduces to 18 %. The model gradient between 70 and 10 m would be weaker than computed here if HNO$_3$ remained in equilibrium with aerosol nitrate, which has low deposition velocity. Measurements by Sievering et al. (1994) over a forest in Germany indicate much weaker vertical gradients for aerosol nitrate than for HNO$_3$, suggesting that equilibrium is not maintained on the short time scales associated with dry deposition.

The remaining model HNO$_3$ bias (18 % annual mean) is driven by an overestimate in winter over the US industrial Midwest. The model has a NMB of 88 % in winter and −14 % in summer. This is similar to the
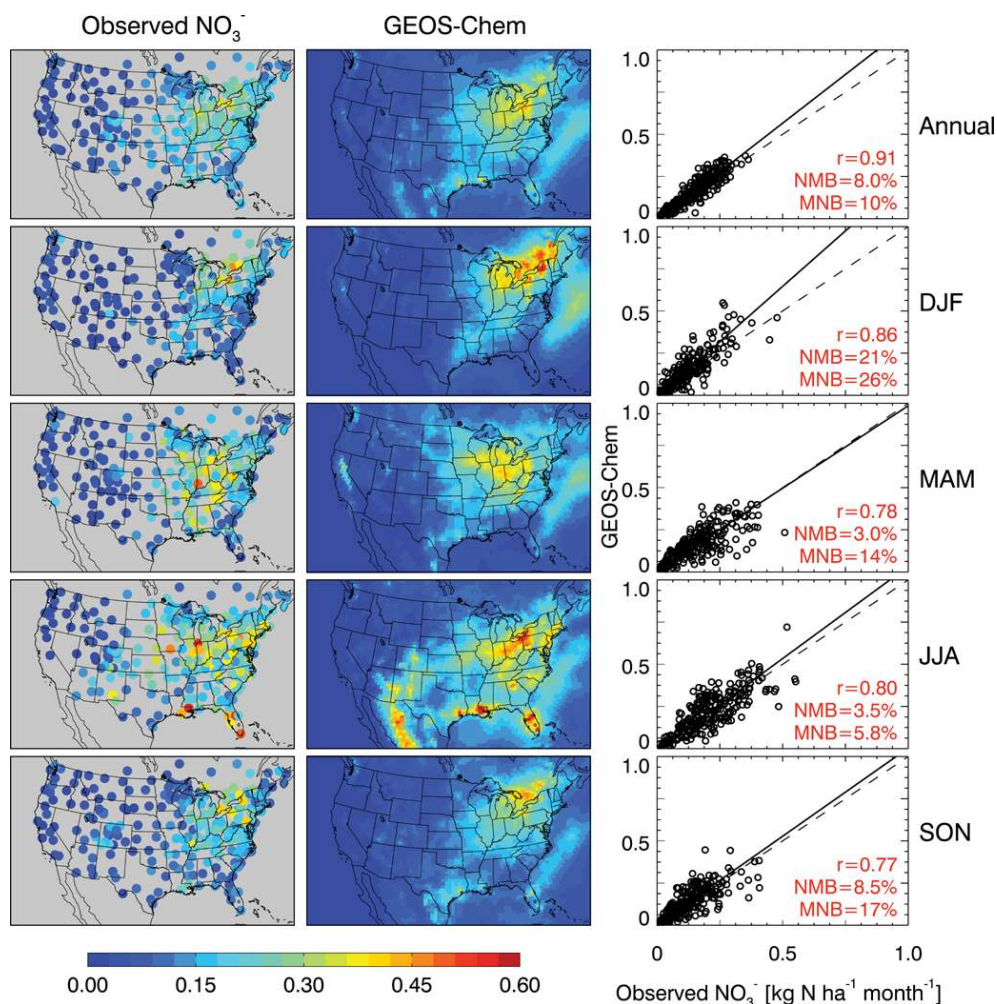
Fig. 3b. Same as Figure 3a but for nitrate (NO_3^-) wet deposition.

previously mentioned model discrepancy with observed nitrate wet deposition fluxes. Model formation of HNO_3 in winter is mostly from heterogeneous N_2O_5 hydrolysis in aerosols (Lamsal et al., 2010) and this process may be overestimated in the standard GEOS-Chem formulation (Evans and Jacob, 2005; Macintyre and Evans, 2010). The aerosol in winter has a large nitrate component, and laboratory studies have shown that $\gamma_{N_2O_5}$ is one order of magnitude smaller for nitrate than for sulfate aerosols because the nitrate inhibits N_2O_5 dissociation (Wahner et al., 1998; Mentel et al., 1999; Bertram and Thornton, 2009). This nitrate inhibition effect is not included in GEOS-Chem. In addition, recent field studies have shown that a significant fraction of nighttime N_2O_5 over the US reacts in chloride-containing aerosols to produce $ClNO_2$, which photolyzes to NO_2 the following morning and hence suppresses HNO_3 formation (Roberts et al., 2009; Thornton et al., 2010).

We further evaluated the model simulation using observed aerosol concentrations of sulfate, nitrate, and ammonium from the CASTNet and EPA Air Quality System sites. Figure 5 compares observed and simulated annual mean values for 2006. The model reproduces the observed annual mean sulfate concentrations ($r = 0.94$–0.96) with only small biases (-4 to -1%). This is important for constraining the model simulation of aerosol nitrate, which can form only if ammonia is in excess of sulfate. Observed ammonium and nitrate concentrations are highest in the Midwest, reflecting agricultural sources of NH_3 that control the formation of ammonium nitrate aerosol. The model has some success in capturing the observed spatial distributions ($r = 0.82$–0.94 for ammonium, 0.60–0.70 for nitrate) but is too high by 17–34% for ammonium and 40–81% for nitrate. The overestimate is most severe over the US Midwest in winter, supporting the hypothesis that HNO_3 formation from N_2O_5 hydrolysis is too high in the model. The HNO_3 overestimate leads more ammonia to partition to the aerosol phase and form ammonium nitrate aerosol.
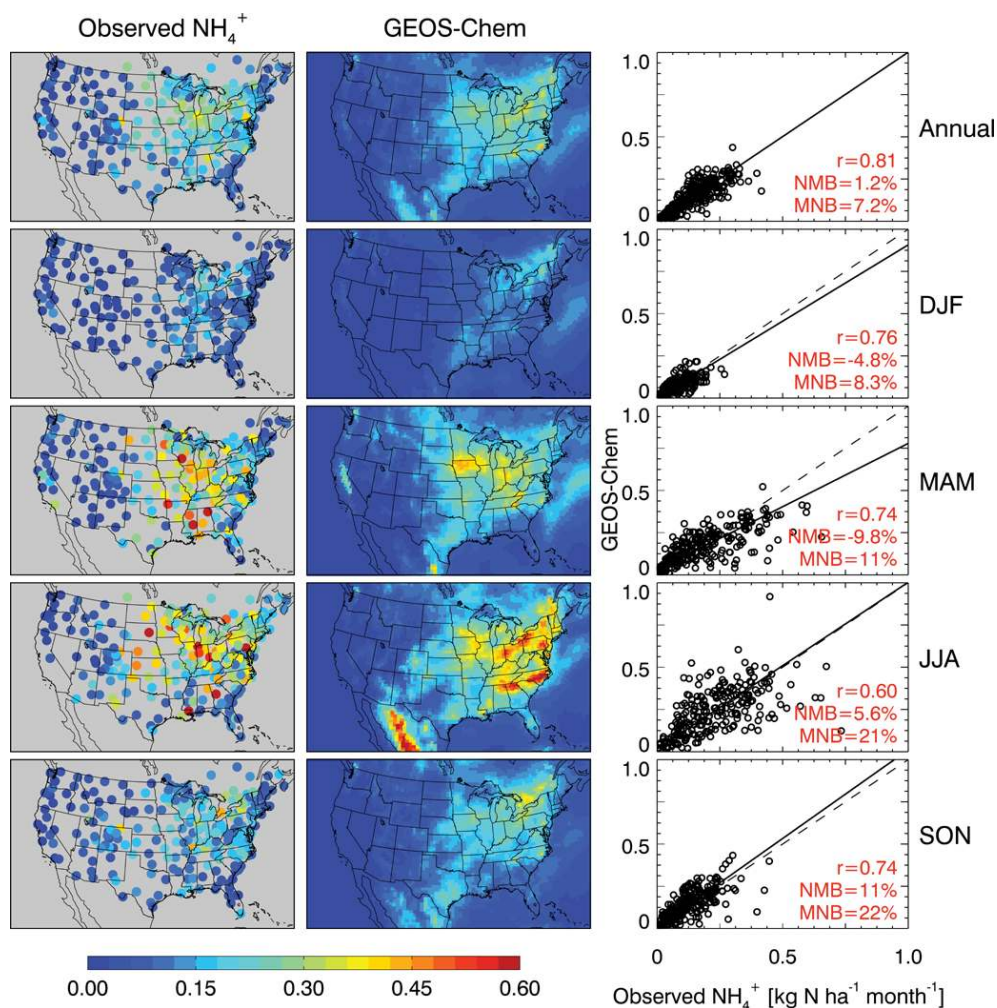
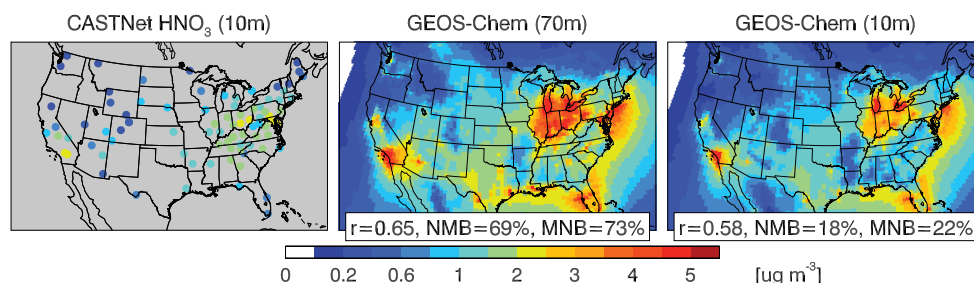**Fig. 3.** Same as Figure 3a but for ammonium (NH_4^+) wet deposition.

Fig. 4. Annual mean HNO_3 concentrations in near-surface air in 2006. Measurements from the CASTNet sites at 10-m altitude (left panel) are compared to GEOS-Chem model values in the lowest model layer (70 m; middle panel). The right panel shows GEOS-Chem HNO_3 concentrations at 10 m inferred from aerodynamic resistances to dry deposition (see text). The correlation coefficients (r), normalized mean biases (NMB), and mean normalized biases (MNB) are shown inset.

Finally, we evaluated the model with NO_2 tropospheric column measurements from the Ozone Monitoring Instrument (OMI) aboard the Aura satellite. This provides an additional check on model NO_x emissions as well as on the lifetime for NO_x oxidation. The OMI NO_2 data (DOMINO v2.0) are from KNMI and are available at http://www.temis.nl (Boersma et al., 2011). Figure 6 compares the OMI tropospheric NO_2 column with GEOS-Chem for March–November 2006. We exclude the winter months due to large OMI retrieval errors over snow (O'Byrne et al., 2010). Model
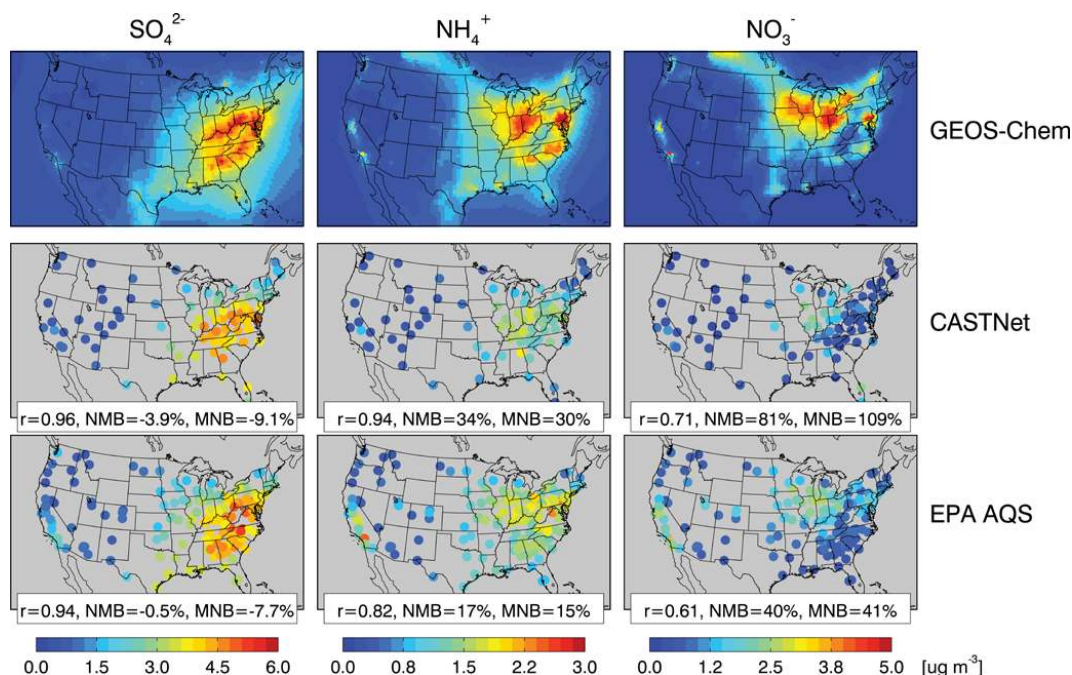
Fig. 5. Annual mean concentrations of sulfate (left), ammonium (middle), and nitrate (right) aerosol in surface air in 2006. Results from the GEOS-Chem model (top) are compared to observations from CASTNet (middle), and EPA AQS (bottom). Statistics for model comparisons to observations are shown inset as correlation coefficients (r), normalized mean biases (NMB), and mean normalized biases (MNB).
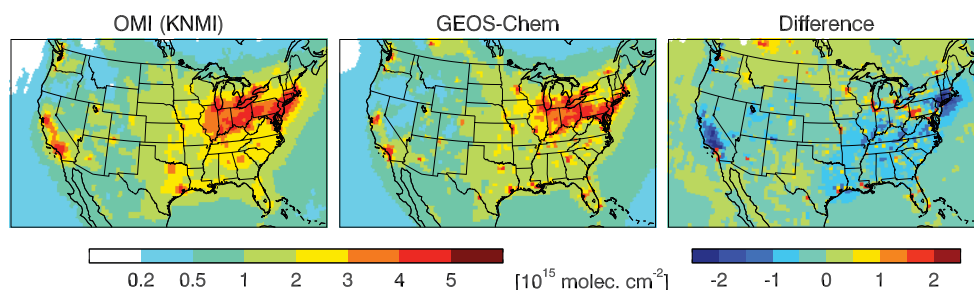

Fig. 6. Mean tropospheric NO_2 columns in March-November 2006. OMI satellite observations mapped on the $1/2° \times 2/3°$ GEOS-Chem grid (left) are compared to GEOS-Chem results (center). The GEOS-Chem minus OMI difference is shown in the right panel.

results are sampled at the satellite overpass time (13:45 local time). The model closely reproduces the spatial distribution of NO_2 tropospheric columns ($r = 0.95$), but there is a mean 12 % low bias over the southeast US and 40 % low bias over California.

4 Nitrogen deposition processes

We now examine the contributions of different processes to nitrogen deposition over the US. We focus here on quantifying the relative contributions from wet vs. dry deposition, from individual nitrogen species, and from domestic anthropogenic vs. other sources. A three-year average of model results (2006–2008) is used to account for interannual variabil-

ity in nitrogen deposition. Relative interannual variability in the model is very small for the results presented here.

Figure 7 shows the annual wet and dry deposition fluxes of oxidized (NO_y) and reduced (NH_x) nitrogen, and Table 3 summarizes the annual total deposition amounts from each process and from individual species over the contiguous US. Dry deposition patterns closely follow emissions (Fig. 1). Wet deposition patterns depend on precipitation as well as on emissions. On the national scale, NO_y is removed preferentially by dry rather than wet deposition (2.9 vs. 1.3 Tg N a^{-1}), while for NH_x dry and wet deposition are comparable (1.0 vs. 1.3 Tg N a^{-1}). The more efficient dry deposition for NO_y reflects the high dry deposition velocity for HNO_3 as shown in Table 1. Annually HNO_3 deposition represents 55 % of NO_y dry deposition, NO_2 22 %, isoprene nitrates 9 %, PAN
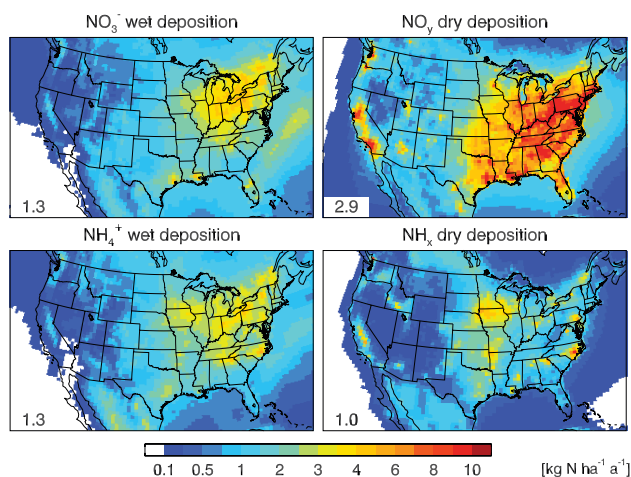
Fig. 7. Simulated annual total fluxes of NO_3^- wet deposition, NO_y dry deposition, NH_4^+ wet deposition, and NH_x dry deposition. Values are 3-year means for 2006-2008. Annual totals over the contiguous US from each process are shown inset in unit of $Tg\,N\,a^{-1}$.

Table 3. Nitrogen deposition over the contiguous US[a].

	Deposition process	Deposition ($Tg\,N\,a^{-1}$)
NO_y	Total	4.2
	Wet NO_3^-	1.3
	Dry HNO_3	1.6
	Dry NO_2	0.64
	Dry isoprene nitrates	0.26
	Dry N_2O_5	0.18
	Dry PANs	0.086
	Dry NO_3^- aerosol	0.068
	Dry alkyl nitrates	0.024
NH_x	Total	2.3
	Wet NH_4^+	1.3
	Dry NH_3	0.83
	Dry NH_4^+ aerosol	0.20

[a] Annual total nitrogen deposition for 2006-2008 computed with the GEOS-Chem model.

3.0 %, and nitrate aerosol 2.3 %. Dry deposition of NH_x is mainly through gaseous NH_3 (82 % of NH_x dry deposition), reflecting its high deposition velocity relative to ammonium aerosol. The previously mentioned CMAQ simulation of Smith and Mueller (2010) simulates an annual NO_y dry deposition flux of $1.9\,Tg\,N\,a^{-1}$ in 2002 over the contiguous United States, with 70 % contributed by HNO_3 dry deposition (J. W. Mallard and S. F. Mueller, personal communication, 2012). Future work is needed to understand the differences between the two models.

Holland et al. (2005) previously estimated annual nitrogen deposition fluxes over the contiguous US from the NADP wet deposition fluxes of nitrate and ammonium, together with the CASTNet-derived dry deposition fluxes of HNO_3, nitrate
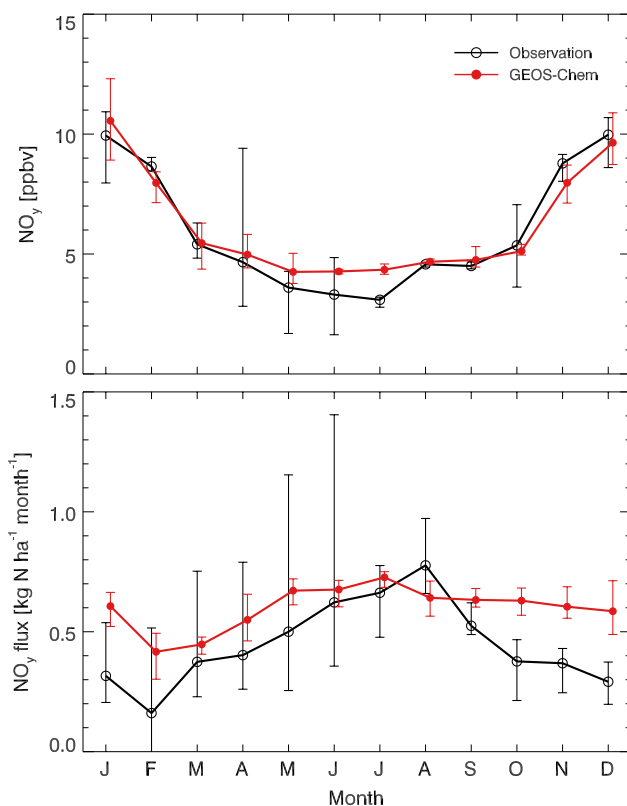

Fig. 8. Monthly NO_y concentrations (top) and dry deposition fluxes (bottom) at Harvard Forest, Massachusetts (42.53° N, 72.18° W). Concentration and eddy covariance flux measurements for 1999-2002 (black) are compared to model results averaged for 2006-2008 (red). The vertical bars indicate the range of the monthly mean values for the four years of measurements and three years of model results.

aerosol, and ammonium aerosol. Their wet deposition fluxes (1.28 and $1.08\,Tg\,N\,a^{-1}$ as NO_y and NH_x respectively) agree closely with our model results, but their dry deposition fluxes (1.20 and $0.18\,Tg\,N\,a^{-1}$ as NO_y and NH_x respectively) are much lower. The differences are in part because the CASTNet data do not account for dry deposition of NO_2, organic nitrates, and NH_3.

Simulated NO_y dry deposition fluxes can be directly compared to eddy covariance NO_y flux measurements at Harvard Forest (42.53° N, 72.18° W), Massachusetts. Figure 8 compares the monthly mean NO_y concentration and eddy covariance flux measurements at Harvard Forest for 1999-2002 to model results for 2006–2008. Measured NO_y concentrations peak in winter and are minimum in summer, with annual means of 6.0–6.2 ppbv. The model reproduces closely the observed values and their seasonal variation. Measured NO_y fluxes peak in summer and are minimum in winter. The model has a weaker seasonality; it captures the summertime fluxes but is too high in fall and winter. The mean measured annual NO_y deposition flux is $5.4\,kg\,N\,ha^{-1}\,a^{-1}$,
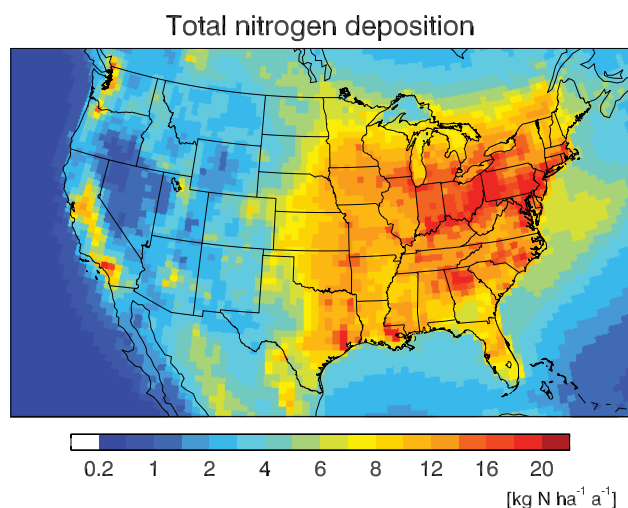
Total nitrogen deposition

Fig. 9. Annual total nitrogen deposition fluxes. Values are GEOS-Chem averages for 2006-2008.

Table 4. Source contributions to nitrogen deposition over the contiguous US[a]

Source	NO_y	NH_x	Total
Anthropogenic			
Domestic	3.4	1.6	5.0
Foreign	0.24	0.18	0.42
Natural	0.57	0.47	1.0

[a] Nitrogen deposition fluxes from different sources computed by the GEOS-Chem model as described in the text. Values are annual total fluxes in unit of $Tg\,N\,a^{-1}$.

5 Domestic, foreign, and natural contributions to nitrogen deposition

Figure 9 shows the simulated spatial distribution of annual total (wet and dry) nitrogen deposition over the US. Nitrogen deposition is generally $>8\,kg\,N\,ha^{-1}\,a^{-1}$ in the eastern US and $1–4\,kg\,N\,ha^{-1}\,a^{-1}$ in remote areas of the west. It is highest in the industrial Midwest with regional values in excess of $15\,kg\,N\,ha^{-1}\,a^{-1}$. Bobbink et al. (1998) and Bouwman et al. (2002) estimate a "critical load" threshold of $10\,kg\,N\,ha^{-1}\,a^{-1}$ for sensitive ecosystems above which disturbance could be significant. In our simulation, 35 % of the US land receives nitrogen deposition exceeding this load.

We separated the contributions to nitrogen deposition from domestic anthropogenic, foreign anthropogenic, and natural sources by conducting sensitivity simulations for 2006 with (1) US domestic NH_3 and NO_x anthropogenic emissions shut off, (2) global anthropogenic emissions shut off. Table 4 summarizes the budgets for the contiguous US. Domestic anthropogenic emissions account respectively for 81 % and 71 % of NO_y and NH_x deposition to the US (78 % of total nitrogen deposition). Foreign anthropogenic emissions contribute 6 % of NO_y deposition, 8 % of NH_x deposition, and 6 % of the total deposition. Natural sources account for the rest: 13 % of NO_y deposition, 21 % of NH_x deposition, and 16 % of total nitrogen deposition.

Figure 10 shows how these deposition enhancements and relative contributions vary by receptor region. The domestic anthropogenic contribution generally exceeds 70 % in the east and in populated areas of the west, falling off to 50–70 % in remote areas of the west. Foreign anthropogenic contributions are generally less than 10 % but can rise up to 30 % near the Canadian and Mexican borders. The rising NO_x and NH_3 emissions from oil production and agriculture in western Canada (Schindler et al., 2006) could significantly affect Montana and North Dakota. Natural source contributions are less than 10 % in the eastern US and the West Coast, and about 20-30 % in the intermountain West, with maximum contributions of 40 % over the southwest US due to lightning emissions and over Idaho due to wildfires.

and the model is 33 % higher ($7.2\,kg\,N\,ha^{-1}\,a^{-1}$). The measured flux was particularly high in 2000 ($8.1\,kg\,N\,ha^{-1}\,a^{-1}$), and had little variation for the other three years ($4.2–4.4\,kg\,N\,ha^{-1}\,a^{-1}$). Model results show little inter-annual variation for 2006-2008 ($6.9–7.5\,kg\,N\,ha^{-1}\,a^{-1}$). The model overestimate of NO_y dry deposition in fall and winter may reflect in large part an excessive N_2O_5 hydrolysis in aerosols, as discussed above. Sparks et al. (2008) measured NO_y eddy flux measurements at Duke Forest (35.97° N, 79.08° W), North Carolina and estimated an annual NO_y dry deposition flux of $4.3\,kg\,N\,ha^{-1}\,a^{-1}$ in 2003. The model is too high ($7.2\,kg\,N\,ha^{-1}\,a^{-1}$) at that site, similar to the comparison at Harvard Forest. However, Sparks et al. (2008) stated that their NO_y eddy flux measurements could be biased low by up to 35 % due to loss of HNO_3 within the instrument inlet.

Eddy covariance flux measurements of PAN have been reported at Duke Forest (Turnipseed et al., 2006), and at Blodgett Forest, California (Wolfe et al., 2009). Turnipseed et al. (2006) found that PAN deposition accounted for 20 % of the daytime NO_y deposition at Duke Forest in July 2003, but Wolfe et al. (2009) found only a 4 % contribution at Blodgett Forest in August-October 2007 after correcting for the PAN thermal decomposition between the altitude of measurement and the surface. We find in GEOS-Chem that PAN contributes respectively 5 % and 4 % of NO_y dry deposition at the two sites in summer.

We find in the model that $4.2\,Tg\,N$ of NO_y and $2.3\,Tg\,N$ of NH_x are deposited annually over the contiguous US. Comparison to US emissions in Table 2 indicates an annual net export of $2.5\,Tg\,N$ as NO_y (38 % of NO_x emissions) and $0.60\,Tg\,N$ as NH_x (21 % of NH_3 emissions). Our results are consistent with Dentener et al. (2006), who found by averaging results from 23 chemical transport models that net export of NO_y from the US amounts to 37 % of US NO_x emissions.
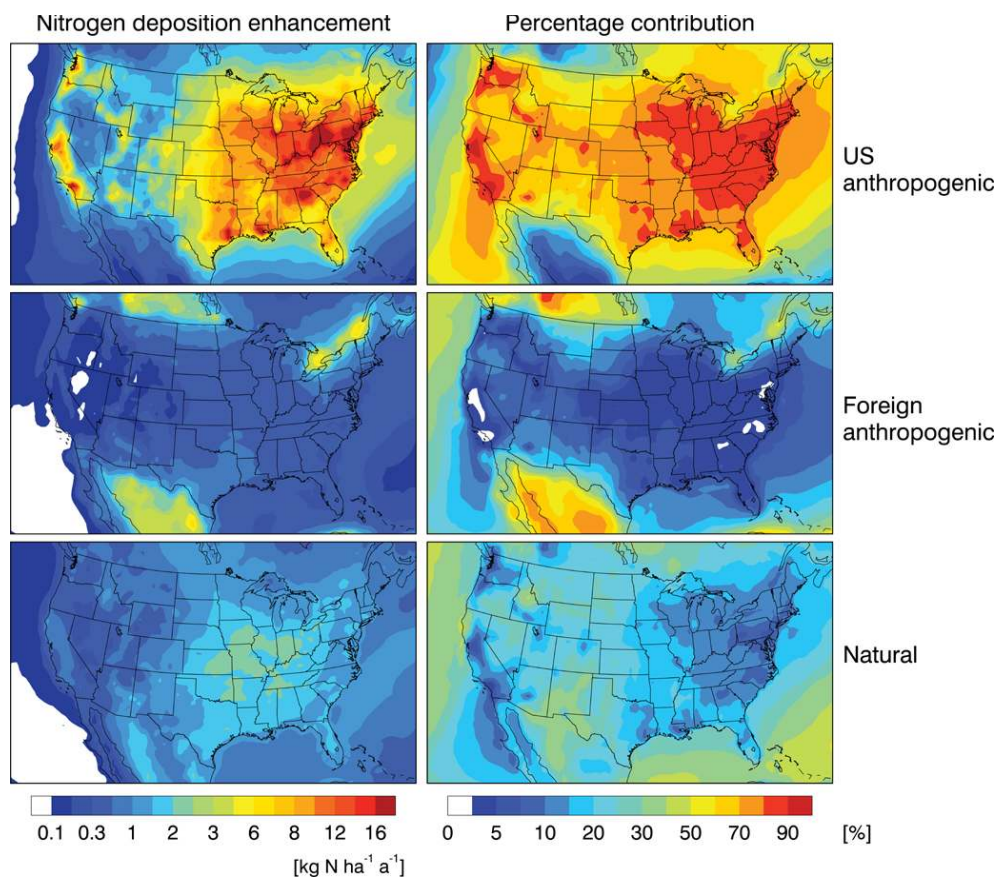
Fig. 10. Domestic anthropogenic, foreign anthropogenic, and natural contributions to annual nitrogen deposition over the contiguous US. Values are from GEOS-Chem sensitivity simulations for 2006 (see text) and are presented as both absolute and relative contributions.

6 Conclusions

We have presented a simulation of nitrogen deposition over the US in 2006–2008 using a nested-grid version of the GEOS-Chem global chemical transport model with $1/2° \times 2/3°$ horizontal resolution over North America and adjacent oceans ($140°$–$40°$ W, $10°$–$70°$ N), and $2° \times 2.5°$ horizontal resolution for the rest of the world. The model includes a detailed representation of oxidant-aerosol chemistry. Our focus was to quantify the processes and species contributing to nitrogen deposition over the contiguous US as well as the relative contributions of domestic anthropogenic, foreign anthropogenic, and natural sources.

Total NO_x and NH_3 emissions in the contiguous US in the model are 6.7 and 2.9 Tg N a^{-1} respectively. Natural sources account for about 20 % annually for both (up to 39 % for NO_x in summer). Previous studies (Gilliland et al., 2003, 2006; Pinder et al., 2006) identified large seasonal biases in US emission inventories for NH_3. Our model imposes a seasonality of NH_3 emissions fitted to surface NH_x measurements from the Midwest RPO and SEARCH networks, such that emissions in winter are about a third those in summer. Successful simulation of observations for NH_x concentrations

and ammonium wet deposition fluxes lends support to the NH_3 emissions used in the model, except in the upper Midwest where emissions appear to be too low.

We evaluated the model with an ensemble of relevant data sets for deposition fluxes and concentrations. The model reproduces the wet deposition fluxes of sulfate, nitrate and ammonium measured at the NADP sites in the US and the CAPMoN sites in Canada with high correlations and no significant bias. Comparison to observed HNO_3 concentrations at CASTNet sites shows a mean positive model bias of 69 %, but we show that this largely reflects the expected concentration gradient between the CASTNet measurement altitude (10 m) and the midpoint of the lowest model layer (70 m). Correcting for this gradient reduces the mean model bias over the US to 18 % and localizes it to the industrial Midwest in winter (88 %). Comparisons with aerosol measurements of sulfate, ammonium and nitrate at CASTNet and EPA-AQS networks show no significant biases for sulfate, but positive biases of 17–34 % for ammonium and 40–81 % for nitrate. The model reproduces closely the spatial pattern of satellite NO_2 tropospheric column measurements from OMI with a 12 % low bias over the Southeast US and 40 % low bias over California. Comparison to multi-year eddy correlation

measurements of NO_y dry deposition fluxes at Harvard Forest, Massachusetts shows good agreement in summer but a factor of 2 high bias in winter.

The main model flaw identified through comparison to the ensemble of observations is excessive HNO_3 production in winter. This production in the model is mainly from N_2O_5 hydrolysis in aerosols, with a mean reactive uptake coefficient $\gamma_{N_2O_5} = 0.003$ averaged across all aerosol types (Evans and Jacob, 2005; Macintyre and Evans, 2010) that is not inconsistent with values inferred from field observations in summer (Brown et al., 2009). However, the model does not account for inhibition of hydrolysis by aerosol nitrate (Davis et al., 2008; Bertram and Thornton, 2009), which would be important in winter when nitrate is a major constituent of the aerosol. It also does not account for reaction of N_2O_5 with chloride aerosol (Roberts et al., 2009; Thornton et al., 2010), which would decrease the HNO_3 yield. These effects should be included in future versions of the model.

We analyzed model results for 2006–2008 to quantify the processes contributing to nitrogen deposition. We find that $6.5\,\text{Tg N a}^{-1}$ is deposited over the contiguous US: $4.2\,\text{Tg N}$ as NO_y and $2.3\,\text{Tg N}$ as NH_x. Dry deposition accounts for 70 % of total deposition for NO_y and 43 % for NH_x. NH_x dry deposition is mainly through NH_3 gas (82 %). Dry deposition of NO_y is partitioned as 55 % HNO_3, 22 % NO_2, 9 % isoprene nitrates, 3.0 % PAN, 2.3 % nitrate aerosol, and 8.7 % other species. The US is a net annual exporter of $2.5\,\text{Tg N}$ as NO_y (38 % of domestic NO_x emissions) and $0.60\,\text{Tg N}$ as NH_x (21 % of domestic NH_3 emissions). Domestic anthropogenic emissions contribute respectively 81 % and 71 % of NO_y and NH_x deposited over the contiguous US, foreign anthropogenic emissions contribute 6 % and 8 %, and natural emissions 13 % and 21 %. The contribution from domestic anthropogenic sources to total nitrogen deposition generally exceeds 70 % in the east and populated areas of the west, and is typically 50–70 % in remote areas of the west. 35 % of the land surface in the contiguous US receives nitrogen deposition in excess of $10\,\text{kg N ha}^{-1}\,\text{a}^{-1}$. A follow-up study will provide a more detailed source attribution of nitrogen deposition in the US.

Edited by: R. Harley

References

Abbatt, J. P. D.: Interaction of HNO_3 with water-ice surfaces at temperatures of the free troposphere, Geophys. Res. Lett., 24, 1479–1482, 1997.

Amos, H. M., Jacob, D. J., Holmes, C. D., Fisher, J. A., Wang, Q., Yantosca, R. M., Corbitt, E. S., Galarneau, E., Rutter, A. P., Gustin, M. S., Steffen, A., Schauer, J. J., Graydon, J. A., Louis, V. L. St., Talbot, R. W., Edgerton, E. S., Zhang, Y., and Sunderland, E. M.: Gas-particle partitioning of atmospheric Hg(II) and its effect on global mercury deposition, Atmos. Chem. Phys., 12, 591–603, doi:10.5194/acp-12-591-2012, 2012.

Aneja, V. P., Chauhan, J. P., and Walker, J. T.: Characterization of atmospheric ammonia emissions from swine waste storage and treatment lagoons, J. Geophys. Res., 105, 11535–11545, 2000.

Asman, W. A. H., Sutton, M. A., and Schjørring, J. K.: Ammonia: emission, atmospheric transport and deposition, New Phytol., 139, 27–48, 1998.

Baughcum, S. L., Tritz, T. G., Henderson, S. C., and Pickett, D. C.: Scheduled Civil Aircraft Emission Inventories for 1992: Database Development and Analysis. NASA Contractor Report 4700, 1996.

Bertram, T. H. and Thornton, J. A.: Toward a general parameterization of N_2O_5 reactivity on aqueous particles: the competing effects of particle liquid water, nitrate and chloride, Atmos. Chem. Phys., 9, 8351–8363, doi:10.5194/acp-9-8351-2009, 2009.

Bertram, T. H., Thornton, J. A., Riedel, T. P., Middlebrook, A. M., Bahreini, R., Bates, T. S., Quinn, P. K., and Coffman, D. J.: Direct observations of N_2O_5 reactivity on ambient aerosol particles, Geophys. Res. Lett., 36, L19803, doi:10.1029/2009gl040248, 2009.

Bey, I., Jacob, D. J., Yantosca, R. M., Logan, J. A., Field, B. D., Fiore, A. M., Li, Q., Liu, H., Mickley, L. J., and Schultz, M. G.: Global modeling of tropospheric chemistry with assimilated meteorology: Model description and evaluation, J. Geophys. Res., 106, 23073–23096, 2001.

Binkowski, F. S. and Roselle, S. J.: Models-3 Community Multiscale Air Quality (CMAQ) model aerosol component: 1. Model description, J. Geophys. Res., 108, 4183, doi:10.1029/2001JD001409, 2003.

Bobbink, R. B., Hornung, M., and Roelofs, J. G. M.: The effects of air-borne nitrogen pollutants on species diversity in natural and semi-natural European vegetation, J. Ecol., 86, 717–738, 1998.

Boersma, K. F., Eskes, H. J., Dirksen, R. J., van der A, R. J., Veefkind, J. P., Stammes, P., Huijnen, V., Kleipool, Q. L., Sneep, M., Claas, J., Leitão, J., Richter, A., Zhou, Y., and Brunner, D.: An improved tropospheric NO_2 column retrieval algorithm for the Ozone Monitoring Instrument, Atmos. Meas. Tech., 4, 1905–1928, doi:10.5194/amt-4-1905-2011, 2011.

Bouwman, A. F., Lee, D. S., Asman, W. A. H., Dentener, F. J., Van Der Hoek, K. W., and Olivier, J. G. J.: A global high resolution emission inventory for ammonia. Global Biogeochem. Cy., 11, 561–587. 1997.

Bouwman, A. F., van Vuuren, D. P., Derwent, R. G., and Posch, M.: A global analysis of acidification and eutrophication of terrestrial ecosystems, Water Air Soil Poll., 141, 349–382, 2002.

Bowman, W. D., Cleveland, C. C., Halada, Å., Hreško, J., and Baron, J. S.: Negative impact of nitrogen deposition on soil buffering capacity, Nat. Geosci., 1, 767–770, doi:10.1038/ngeo339, 2008.

Brown, S. S., Dubé, W. P., Fuchs, H., Ryerson, T. B., Wollny, A. G., Brock, C. A., Bahreini, R., Middlebrook, A. M., Neuman, J. A., Atlas, E., Roberts, J. M., Osthoff, H. D., Trainer, M., Fehsenfeld, F. C., and Ravishankara, A. R.: Reactive uptake coefficients for N2O5determined from aircraft measurements during the Second Texas Air Quality Study: Comparison to current model parameterizations, J. Geophys. Res., 114, D00F10, doi:10.1029/2008jd011679, 2009.

Businger, J. A., Wyngaard, J. C., Izumi, Y., and Bradley, E. F.: Flux-profile relationships in the atmospheric surface layer, J. Atmos. Sci., 28, 181–189, 1971.

Chen, D., Wang, Y. X., McElroy, M. B., He, K., Yantosca, R. M., and Le Sager, P.: Regional CO pollution in China simulated by high-resolution nested-grid GEOS-Chem model, Atmos. Chem. Phys., 11, 3825–3839, doi:10.5194/acp-11-3825-2009, 2009.

Clarke, J. F., Edgerton, E. S., and Martin, B. E.: Dry deposition calculations for the Clean Air Status and Trends Network, Atmos. Environ., 31, 3667–3678, 1997.

Davis, J. M., Bhave, P. V., and Foley, K. M.: Parameterization of N_2O_5 reaction probabilities on the surface of particles containing ammonium, sulfate, and nitrate, Atmos. Chem. Phys., 8, 5295–5311, doi:10.5194/acp-8-5295-2008, 2008.

Dentener, F., Drevet, J., Lamarque, J. F., Bey, I., Eickhout, B., Fiore, A. M., Hauglustaine, D., Horowitz, L. W., Krol, M., Kulshrestha, U. C., Lawrence, M., Galy-Lacaux, C., Rast, S., Shindell, D., Stevenson, D., Van Noije, T., Atherton, C., Bell, N., Bergman, D., Butler, T., Cofala, J., Collins, B., Doherty, R., Ellingsen, K., Galloway, J., Gauss, M., Montanaro, V., Müller, J. F., Pitari, G., Rodriguez, J., Sanderson, M., Solmon, F., Strahan, S., Schultz, M., Sudo, K., Szopa, S., and Wild, O.: Nitrogen and sulfur deposition on regional and global scales: A multimodel evaluation, Global Biogeochem. Cy., 20, GB4003, doi:10.1029/2005GB002672, 2006.

Doskey, P. V., Kotamarthi, V. R., Fukui, Y., Cook, D. R., Breitbeil III, F. W., and Wesely, M. L.: Air-surface exchange of peroxyacetyl nitrate at a grassland site, J. Geophys. Res., 109, D10310, doi:10.1029/2004JD004533, 2004.

Edgerton, E., Saylor, R., Hartsell, B., Jansen, J., and Alanhansen, D.: Ammonia and ammonium measurements from the southeastern United States, Atmos. Environ., 41, 3339-3351, doi:10.1016/j.atmosenv.2006.12.034, 2007.

Ellis, R. A., Murphy, J. G., Markovic, M. Z., VandenBoer, T. C., Makar, P. A., Brook, J., and Mihele, C.: The influence of gas-particle partitioning and surface-atmosphere exchange on ammonia during BAQS-Met, Atmos. Chem. Phys., 11, 133–145, doi:10.5194/acp-11-133-2011, 2011.

Evans, M. J. andJacob, D. J.: Impact of new laboratory studies of N2O5 hydrolysis on global model budgets of tropospheric nitrogen oxides, ozone, and OH, Geophys. Res. Lett., 32, L09813, doi:10.1029/2005gl022469, 2005.

Fisher, J. A., Jacob, D. J., Wang, Q., Bahreini, R., Carouge, C. C., Cubison, M. J., Dibb, J. E., Diehl, T., Jimenez, J. L., Leibensperger, E. M., Lu, Z., Meinders, M. B. J., Pye, H. O. T., Quinn, P. K., Sharma, S., Streets, D. G., van Donkelaar, A., and Yantosca, R. M.: Sources, distribution, and acidity of sulfate-ammonium aerosol in the Arctic in winter-spring, Atmos. Environ., 45, 7301–7318, doi:10.1016/j.atmosenv.2011.08.030, 2011.

Galloway, J. N., Dentener, F. J., Capone, D. G., Boyer, E. W., Howarth, R. W., Seitzinger, S. P., Asner, G. P., Cleveland, C. C.,

Green, P. A., Holland, E. A., Karl, D. M., Michaels, A. F., Porter, J. H., Townsend, A. R., and Vorosmarty, C. J.: Nitrogen cycles: past, present, and future, Biogeochem., 70, 153–226, 2004.

Geigert, M. A., Nikolaidis, N. P., Miller, D. R., and Heitert, J.: Deposition rates for sulfur and nitrogen to a hardowood forest in northern Connecticut, USA, Atmos. Environ., 28, 1689–1697, 1994.

Gilliland, A. B., Dennis, R. L., Roselle, S. J., and Pierce, T. E.: Seasonal NH3 emission estimates for the eastern United States based on ammonium wet concentrations and an inverse modeling method, J. Geophys. Res., 108, D15, 4477, doi:10.1029/2002jd003063, 2003.

Gilliland, A. B., Wyat Appel, K., Pinder, R. W., and Dennis, R. L.: Seasonal NH3 emissions for the continental United States: Inverse model estimation and evaluation, Atmos. Environ., 40, 4986–4998, 2006.

Guenther, A., Karl, T., Harley, P., Wiedinmyer, C., Palmer, P. I., and Geron, C.: Estimates of global terrestrial isoprene emissions using MEGAN (Model of Emissions of Gases and Aerosols from Nature), Atmos. Chem. Phys., 6, 3181–3210, doi:10.5194/acp-6-3181-2006, 2006.

Hicks, B.: Dry deposition to forests – On the use of data from clearings, Agr. Forest Meteorol., 136, 214–221, doi:10.1016/j.agrformet.2004.06.013, 2006.

Holland, E. A., Bradswell, B. H., Sulzman, J., and Lamarque, J.-F.: Nitrogen Deposition onto the United States and Western Europe: Synthesis of Observations and Models, Ecol. Appl., 15, 38–57, 2005.

Horii, C. V., William Munger, J., Wofsy, S. C., Zahniser, M., Nelson, D., and Barry McManus, J.: Atmospheric reactive nitrogen concentration and flux budgets at a Northeastern U.S. forest site, Agr. Forest Meteorol., 133, 210–225, 2005.

Horowitz, L. W., Liang, J., Gardner, G., and Jacob, D. J.: Export of reactive nitrogen from North America during summertime: Sensitivity to hydrocarbon chemistry, J. Geophys. Res., 103, 13451–13476, 1998.

Hudman, R. C., Jacob, D. J., Turquety, S., Leibensperger, E. M., Murray, L. T., Wu, S., Gilliland, A. B., Avery, M., Bertram, T. H., Brune, W., Cohen, R. C., Dibb, J. E., Flocke, F. M., Fried, A., Holloway, J., Neuman, J. A., Orville, R., Perring, A., Ren, X., Sachse, G. W., Singh, H. B., Swanson, A., and Wooldridge, P. J.: Surface and lightning sources of nitrogen oxides over the United States: Magnitudes, chemical evolution, and outflow, J. Geophys. Res., 112, D12S05, doi:10.1029/2006jd007912, 2007.

Jacob, D. J.: Heterogeneous chemistry and tropospheric ozone, Atmos. Environ., 34, 2131–2159, 2000.

Jacob, D. J., Logan, J. A., Gardner, G. M., Yevich, R. M., Spivakovsky, C. M., Wofsy, S. C., Sillman, S., and Prather, M. J.: Factors Regulating Ozone Over the United States and Its Export to the Global Atmosphere, J. Geophys. Res., 98, 14817–14826, doi:10.1029/98jd01224, 1993.

Kasibhatla, P. S., Levy Ii, H., and Moxim, W. J.: GLobal NOx, HNO3, PAN, and NOy distrubtions from fossil fuel combustion emissions: A model study, J. Geophys. Res., 98, 7165–7180, 1993.

Kuhns, H., Knipping, E. M., and Vukovich, J. M.: Development of a United States-Mexico emissions inventory for the Big Bend Regional Aerosol and Visibility Observational (BRAVO) Study, J. Air Waste Manage., 55, 677–692, 2005.

Lamsal, L. N., Martin, R. V., van Donkelaar, A., Celarier, E. A., Bucsela, E. J., Boersma, K. F., Dirksen, R., Luo, C., and Wang, Y.: Indirect validation of tropospheric nitrogen dioxide retrieved from the OMI satellite instrument: Insight into the seasonal variation of nitrogen oxides at northern midlatitudes, J. Geophys. Res., 115, D05302, doi:10.1029/2009jd013351, 2010.

Lerdau, M. T., Munger, J. W., Jacob, D. J.: The NO_2 flux conundrum, Science, 289, 2291–2293, 2000.

Li, Q., Jacob, D. J., Munger, J. W., Yantosca, R. M., and Parrish, D. D.: Export of NO_y from the North American boundary layer: Reconciling aircraft observations and global model budgets, J. Geophys. Res., 109, D02313, doi:10.1029/2003jd004086, 2004.

Liang, J., Horowitz, L. W., Jacob, D. J., Wang, Y., Fiore, A. M., Logan, J. A., Gardner, G. M., and Munger, J. W.: Seasonal budgets of reactive nitrogen species and ozone over the United States, and export fluxes to the global atmosphere, J. Geophys. Res., 103, 13435–13450, 1998.

Liu, H. Y., Jacob, D. J., Bey, I., and Yantosca, R. M.: Constraints from Pb-210 and Be-7 on wet deposition and transport in a global three-dimensional chemical tracer model driven by assimilated meteorological fields, J. Geophys. Res., 106, 12109–12128, 2001.

Macintyre, H. L. and Evans, M. J.: Sensitivity of a global model to the uptake of N_2O_5 by tropospheric aerosol, Atmos. Chem. Phys., 10, 7409–7414, doi:10.5194/acp-10-7409-2010, 2010.

Mao, J., Jacob, D. J., Evans, M. J., Olson, J. R., Ren, X., Brune, W. H., Clair, J. M. S., Crounse, J. D., Spencer, K. M., Beaver, M. R., Wennberg, P. O., Cubison, M. J., Jimenez, J. L., Fried, A., Weibring, P., Walega, J. G., Hall, S. R., Weinheimer, A. J., Cohen, R. C., Chen, G., Crawford, J. H., McNaughton, C., Clarke, A. D., Jaeglé, L., Fisher, J. A., Yantosca, R. M., Le Sager, P., and Carouge, C.: Chemistry of hydrogen oxide radicals (HO_x) in the Arctic troposphere in spring, Atmos. Chem. Phys., 10, 5823–5838, doi:10.5194/acp-10-5823-2010, 2010.

Mari, C., Jacob, D. J., and Bechtold, P.: Transport and scavenging of soluble gases in a deep convective cloud, J. Geophys. Res., 105, 22255– 22267, 2000.

Martin, R. V., Jacob, D. J., Yantosca, R. M., Chin, M., and Ginoux, P.: Global and regional decreases in tropospheric oxidants from photochemical effects of aerosols, J. Geophys. Res., 108, 4097, doi:10.1029/2002JD002622, 2003.

Martin, R. V., Sauvage, B., Folkins, I., Sioris, C. E., Boone, C., Bernath, P., and Ziemke, J.: Space-based constraints on the production of nitric oxide by lightning, J. Geophys. Res., 112, D09309, doi:10.1029/2006jd007831, 2007.

Mentel, T. F., Sohn, M., and Wahner, A.: Nitrate effect in the heterogeneous hydrolysis of dinitrogen pentoxide on aqueous aerosols, Phys. Chem. Chem. Phys., 1, 5451–5457, doi:10.1039/a905338g, 1999.

O'Byrne, G., Martin, R. V., van Donkelaar, A., Joiner, J., and Celarier, E. A.: Surface reflectivity from the Ozone Monitoring Instrument using the Moderate Resolution Imaging Spectroradiometer to eliminate clouds: Effects of snow on ultraviolet and visible trace gas retrievals, J. Geophys. Res., 115, D17305, doi:10.1029/2009JD013079, 2010.

Olivier, J. G. J., Berdowski, J. J. M.: Global emissions sources and sinks, in: The Climate System, edited by: Berdowski, J., Guicherit, R., and Heij, B. J., 33–78, A.A. Balkema Publishers/Swets & Zeitlinger Publishers, Lisse, The Netherlands, 2001.

Park, R. J., Jacob, D. J., Field, B. D., Yantosca, R. M., and Chin, M.: Natural and transboundary pollution influences on sulfate-nitrate-ammonium aerosols in the United States: Implications for policy, J. Geophys. Res., 109, D15204, doi:10.1029/2003jd004473, 2004.

Pickering, K. E., Wang, Y. S., Tao, W. K., Price, C., and Muller J. F.: Vertical distributions of lightning NOx for use in regional and global chemical transport models. J. Geophys. Res., 103, 31203–31216, 1998.

Pinder, R. W., Adams, P. J., Pandis, S. N., and Gilliland, A. B.: Temporally resolved ammonia emission inventories: Current estimates, evaluation tools, and measurement needs, J. Geophys. Res., 111, D16310, doi:10.1029/2005jd006603, 2006.

Price, C. and Rind, D.: A simple lightning parameterization for calculating global lightning distributions, J. Geophys. Res. 97, 9919–9933, 1992.

Reay, D. S., Dentener, F., Smith, P., Grace, J., and Feely, R. A.: Global nitrogen deposition and carbon sinks, Nat. Geosci., 1, 430–437, 2008,

Roberts, J. M., Osthoff, H. D., Brown, S. S., Ravishankara, A. R., Coffman, D., Quinn, P., and Bates, T.: Laboratory studies of products of N_2O_5 uptake on Cl-containing substrates, Geophys. Res. Lett., 36, L20808, doi:10.1029/2009gl040448, 2009.

Sanderson, M. G., Dentener, F. J., Fiore, A. M., Cuvelier, C., Keating, T. J., Zuber, A., Atherton, C. S., Bergmann, D. J., Diehl, T., Doherty, R. M., Duncan, B. N., Hess, P., Horowitz, L. W., Jacob, D. J., Jonson, J. E., Kaminski, J. W., Lupu, A., MacKenzie, I. A., Mancini, E., Marmer, E., Park, R., Pitari, G., Prather, M. J., Pringle, K. J., Schroeder, S., Schultz, M. G., Shindell, D. T., Szopa, S., Wild, O., and Wind, P.: A multi-model study of the hemispheric transport and deposition of oxidised nitrogen, Geophys. Res. Lett., 35, L17815, doi:10.1029/2008GL035389, 2008.

Sauvage, B., Martin, R. V., van Donkelaar, A., Liu, X., Chance, K., Jaeglé, L., Palmer, P. I., Wu, S., and Fu, T.-M.: Remote sensed and in situ constraints on processes affecting tropical tropospheric ozone. Atmos. Chem. Phys. 7, 815–838, doi:10.5194/acp-7-815-2007, 2007.

Schindler, D. W., Dillon, P. J., and Schreier, H.: A review of anthropogenic sources of nitrogen and their effects on Canadian aquatic ecosystems, Biogeochemistry, 79, 25–44, doi:10.1007/s10533-006-9001-2, 2006.

Sievering, H., Enders, G., Kins, L., Kramm, G., Ruoss, K., Roider, G., Zelger, M., Anderson, L., and Dlugi, R.: Nitric acid, particulate nitrate and ammonium profiles at the Bayerischer Wald: evidence for large deposition rates of total nitrate, Atmos. Environ., 28, 311–315, 1994.

Sievering, H., Kelly, T., McConville, G., Seibold, C., and Turnipseed, A.: Nitric acid dry deposition to conifer forests: Niwot Ridge spruce-fir-pine study. Atmos. Environ., 35, 3851–3859, 2001.

Smith, S. N., and Mueller, S. F.: Modeling natural emissions in the Community Multiscale Air Quality (CMAQ) Model-I: building an emissions data base, Atmos. Chem. Phys., 10, 4931-4952, 2010,
http://www.atmos-chem-phys.net/10/4931/2010/.

Stevens, C. J., Dise, N. B., Mountford, J. O., and Gowing, D. J.: Impact of nitrogen deposition on the species richness of grasslands, Science, 303, 1876–1879, 2004.

Sutton, M. A., Burkhardt, J. K., Guerin, D., Nemitz, E., and Fowler, D.: Development of resistance models to describe measurements of bi-directional ammonia surface-atmosphere exchange, Atmos. Environ., 32, 473–480, 1998.

Thornton, J. A., Kercher, J. P., Riedel, T. P., Wagner, N. L., Cozic, J., Holloway, J. S., Dubé, W. P., Wolfe, G. M., Quinn, P. K., Middlebrook, A. M., Alexander, B., and Brown, S. S.: A large atomic chlorine source inferred from mid-continental reactive nitrogen chemistry, Nature, 464, 271–274, doi:10.1038/nature08905, 2010.

Turnipseed, A. A., Huey, L. G., Nemitz, E., Stickel, R., Higgs, J., Tanner, D. J., Slusher, D. L., Sparks, J. P., Flocke, F., and Guenther, A.: Eddy covariance fluxes of peroxyacetyl nitrates (PANs) and NO$_y$ to a coniferous forest, J. Geophys. Res., 111, D09304, doi:10.1029/2005jd006631, 2006.

US EPA (Environmental Protection Agency): Integrated Science Assessment (ISA) f Oxides of Nitrogen and Sulfur–Ecological Criteria (Final Report). EPA/600/R-08/082F, US Environmental Prot Assessment–RTP Division, Office of Research and Development, Research Triangle Park, NC, USA, available at http://cfpub.epa.gov/ncea/cfm/recordisplay.cfm?deid=201485, 2008.

van der Werf, G. R., Randerson, J. T., Giglio, L., Collatz, J. G., Kasibhatla, P., and Arellano, A. F.: Interannual variability in global biomass burning emissions from 1997 to 2004, Atmos. Chem. Phys., 6, 3423–3441, doi:10.5194/acp-6-3423-2006, 2006.

van Donkelaar, A., Martin, R. V., Leaitch, W. R., Macdonald, A. M., Walker, T. W., Streets, D. G., Zhang, Q., Dunlea, E. J., Jimenez, J. L., Dibb, J. E., Huey, L. G., Weber, R., and Andreae, M. O.: Analysis of aircraft and satellite measurements from the Intercontinental Chemical Transport Experiment (INTEX-B) to quantify long-range transport of East Asian sulfur to Canada, Atmos. Chem. Phys., 8, 2999–3014, doi:10.5194/acp-8-2999-2008, 2008.

Vestreng, V. and Klein, H.: Emission data reported to UNECE/EMEP. Quality assurance and trend analysis and Presentation of WebDab, MSC-W Status Report 2002, Norwegian Meteorological Institute, Oslo, Norway, 2002.

Vitousek, P. M., Aber, J. D., Howarth, R. W., Likens, G. E., Matson, P. A., Schindler, D. W., Schlesinger, W. H., and Tillman, D. G.: Human alteration of the global nitrogen cycle: Sources and consequences, Ecol. Appl., 7, 737–750. 1997.

Wahner, A., Mentel, T. F., Sohn, M., and Stier, J.: Heterogeneous reaction of N$_2$O$_5$ on sodium nitrate aerosol, J. Geophys. Res., 103, 31103–31112, 1998.

Wang, J., Hoffmann, A. A., Park, R. J., Jacob, D. J., and Martin, S. T.: Global distribution of solid and aqueous sulfate aerosols: Effect of the hysteresis of particle phase transitions, J. Geophys. Res., 113, D11206, doi:10.1029/2007jd009367, 2008.

Wang, Y. H., Jacob, D. J., and Logan, J. A.: Global simulation of tropospheric O$_3$-NO$_x$-hydrocarbon chemistry, J. Geophys. Res., 103, 10713–10725, 1998.

Wang, Y. X., McElroy, M. B., Jacob, D. J., and Yantosca, R. M.: A nested grid formulation for chemical transport over Asia: Applications to CO, J. Geophys. Res., 109, D22307, doi:10.1029/2004jd005237, 2004.

Wesely, M. L.: Parameterization of surface resistances to gaseous dry deposition in regional-scale numerical-models, Atmos. Environ., 23, 1293–1304, 1989.

Wolfe, G. M., J. A. Thornton, R. L. N. Yatavelli, et al., Eddy covariance fluxes of acyl peroxy nitrates (PAN, PPN and MPAN) above a Ponderosa pine forest, Atmos. Chem. Phys., 9, 615–635, doi:10.5194/acp-9-615-2009, 2009.

Yienger, J. J. and Levy II, H.: Empirical model of global soil biogenic NO$_x$ emissions, J. Geophys. Res., 100, 11447–11464, 1995.

Zhang, L., Jacob, D. J., Downey, N. V., Wood, D. A., Blewitt, D., Carouge, C. C., van Donkelaar, A., Jones, D. B. A., Murray, L. T., and Wang, Y.: Improved estimate of the policy-relevant background ozone in the United States using the GEOS-Chem global model with 1/2° ×2/3° horizontal resolution over North America, Atmos. Environ., 45, 6769–6776, doi:10.1016/j.atmosenv.2011.07.054, 2011.

Zhang, Q., Streets, D. G., Carmichael, G. R., He, K. B., Huo, H., Kannari, A., Klimont, Z., Park, I. S., Reddy, S., Fu, J. S., Chen, D., Duan, L., Lei, Y., Wang, L. T., and Yao, Z. L.: Asian emissions in 2006 for the NASA INTEX-B mission, Atmos. Chem. Phys., 9, 5131–5153, doi:10.5194/acp-9-5131-2009, 2009.